

Supplementary figures:

Figure S1– Activity (in U/mg) vs. pH profiles for SDH^{WT}, SDH^{Y236F}, SDH^{R55M}, SDH^{H57A} recorded using standard assay conditions, i.e. 2 mM sulfite and 0.04 mM cytochrome *c* (horse heart).

Figure S2 – Stopped Flow data for the reductive half reaction of SDH^{H57A} – plots of reaction rates (s⁻¹) collected at different pH values vs. sulfite concentration are shown. Filled circles (●) – pH 6, open circles (○) – pH 7, filled triangles (▼) – pH 8, open triangles (△) – pH 9. The increase in reaction rate with increasing sulfite concentrations, which is maximal for data collected at pH 7, reflects the magnitude of k_d sulfite. The data mirror the behavior of the steady-state parameter $K_{M \text{ sulfite app}}$.

Figure S3 - Comparison of the X-band CW EPR (trace 1) and Ka-band ESE field sweep (trace 2, numerical first derivative) of SDH^{H57A} shows that the features seen at the high-field side of the EPR spectrum are caused by the presence of centers with different g-tensors, and not by the *hfi*. Experimental conditions for trace 1: mw frequency, 9.461 GHz; mw power, 200 μW; modulation amplitude, 0.2 mT; temperature, 77 K. Experimental conditions for trace 2: mw frequency, 29.566 GHz; mw pulses, 2×80 ns (two-pulse sequence); time interval between the mw pulses, $\tau = 300$ ns; boxcar integration gate, 150 ns; temperature, 21 K.

Figure S4 - Refocused ¹H Mims ENDOR spectra of SDH^{H57A} at different EPR positions, as indicated in the Figure. Experimental conditions: mw frequency, 29.566 GHz; mw pulses, 3×13 ns + 20 ns; time interval between the first two mw pulses, $\tau = 80$ ns; time interval between the second and the third mw pulses, $T = 30$ μs; RF pulse length, 20 μs; stochastic RF sweep; temperature, 21 K. The bottom spectrum is recorded at the high-field side of the spectrum where only Species II with the lowest g_x is contributing. The narrow features with splittings ≤ 4 MHz in all spectra are mostly contributed to by the non-exchangeable protons belonging to the protein. The broad features with splittings > 4 MHz are characteristic of an exchangeable proton of the equatorial OH ligand (34). The broad feature under the more narrow central lines comes from the proton of the equatorial OH ligand. This shows that the Mo(V) center of Species II has essentially the same structure as that of Species I (usual *hpH*-type center).

Figure S5

Stereo views of electron density around the Mo active site showing the molybdenum cofactor surrounded by residues Arg55, His57, Cys104 and Tyr236. **A.** R55M substituted enzyme with bound sulfate contoured at 1.5s. **B.** H57A substituted enzyme demonstrating disordered R55 contoured at 1.2s. **C.** Y236F substituted enzyme demonstrating slightly disordered R55 contoured at 1.2s. **D.** Wild-type enzyme contoured at 1.5s. All maps were calculated using data to 2 Å.

Table S1 - Stability of SDH^{WT} following pre-incubation at different pH values. Purified SDH^{WT} was diluted into buffers of the specified pH. Three individual dilutions were set up for each pH. Samples were taken from these buffers at specified times and immediately used in standard SDH assays at pH 8.0. The data is shown as μ moles sulfite oxidized per minute in the assay. Similar data was collected for SDH^{R55M} and SDH^{H57A} at pH 6.0, 8.0 and 10.0 (data not shown) and also showed that on the timescale of a standard SDH assay (1-2 minutes) the enzyme is stable at all pH values used in this study.

Time (min)	pH 6.0	pH 7.0	pH 8.0	pH 9.0	pH 10.0
0	0.0162	0.0149	0.0177	0.0142	0.0152
5	0.0158	0.0146	0.0165	0.0145	0.0174
10	0.0175	0.0144	0.0183	0.0146	0.0198
15	0.0197	0.0151	0.0165	0.0144	0.0172

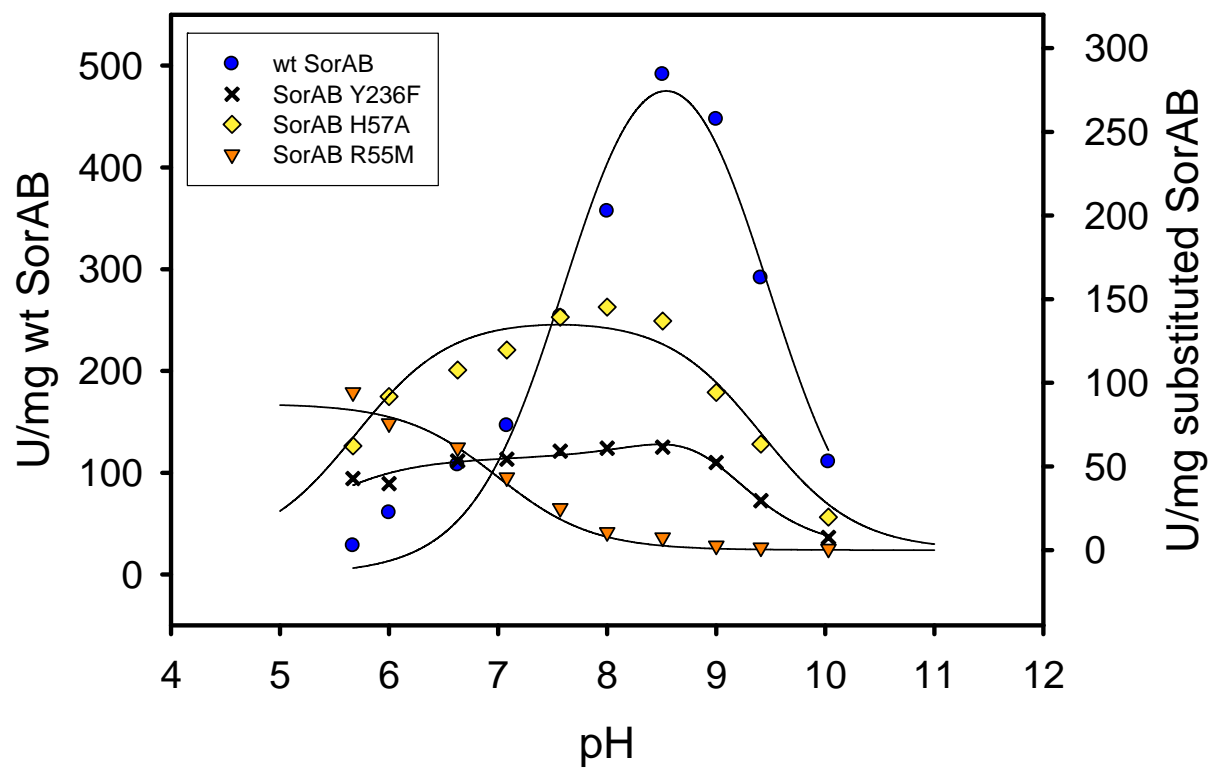


Figure S1

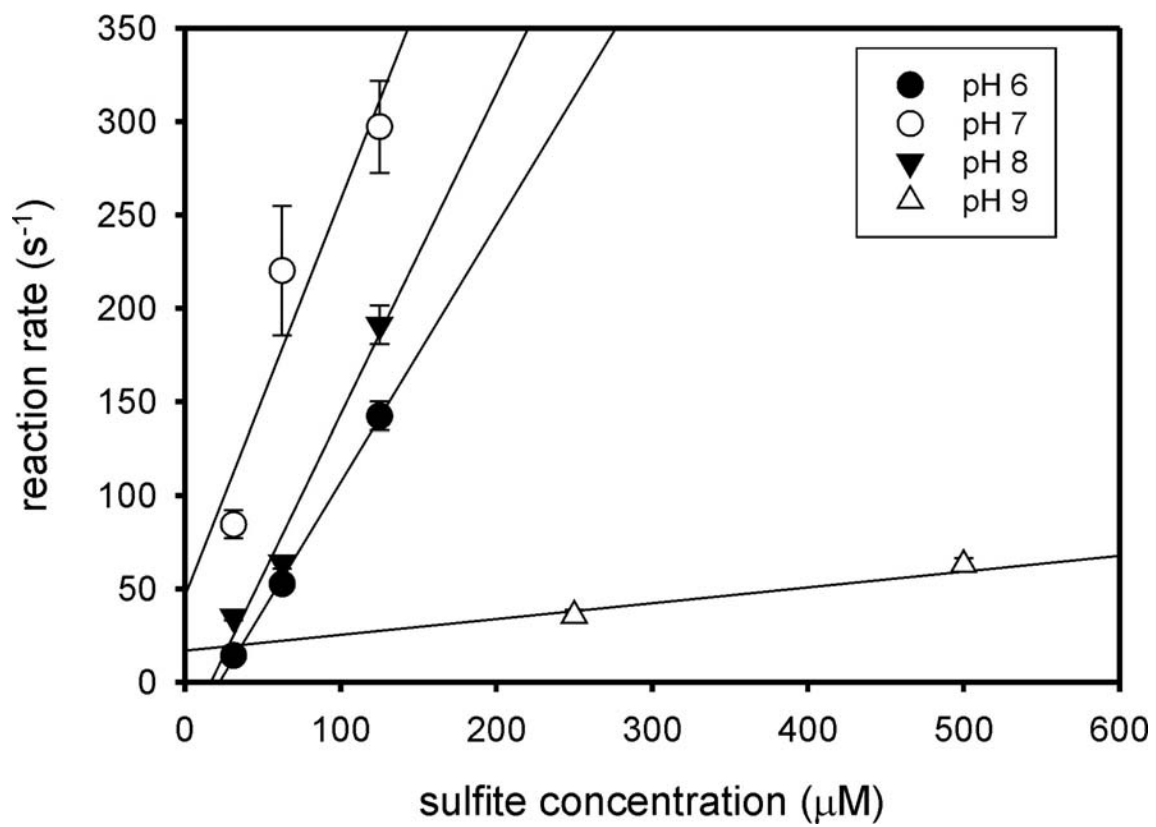


Figure S2

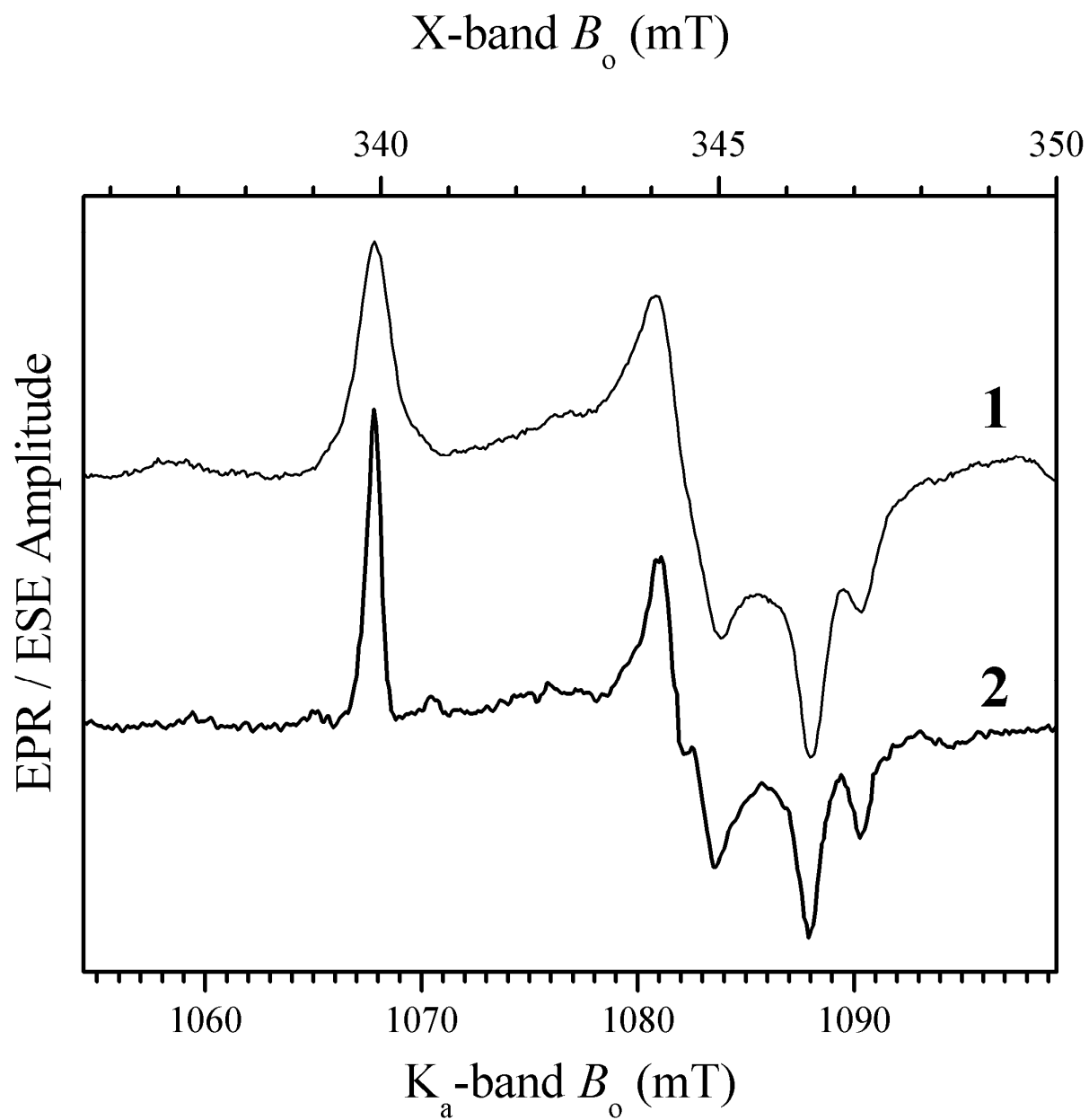


Figure S3

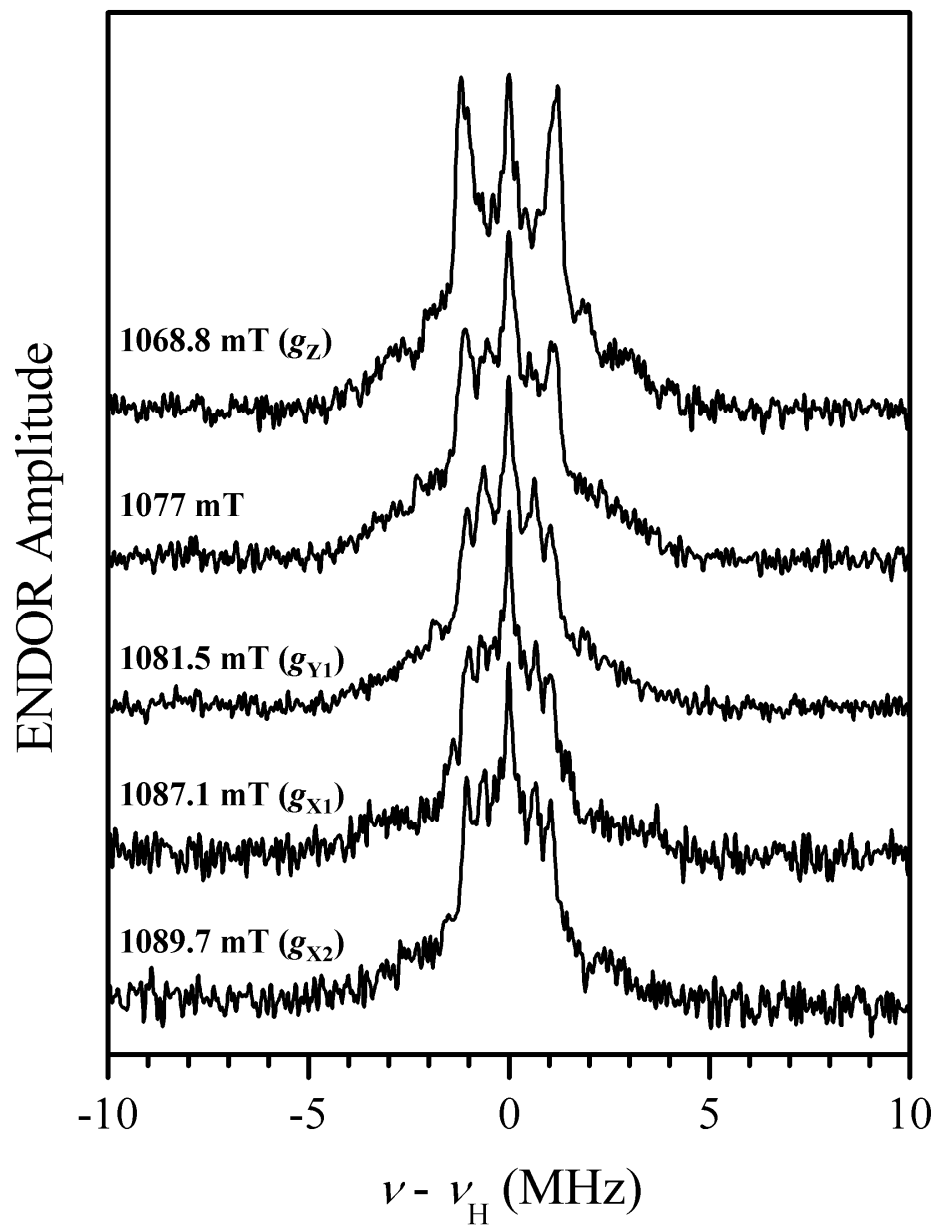


Figure S4

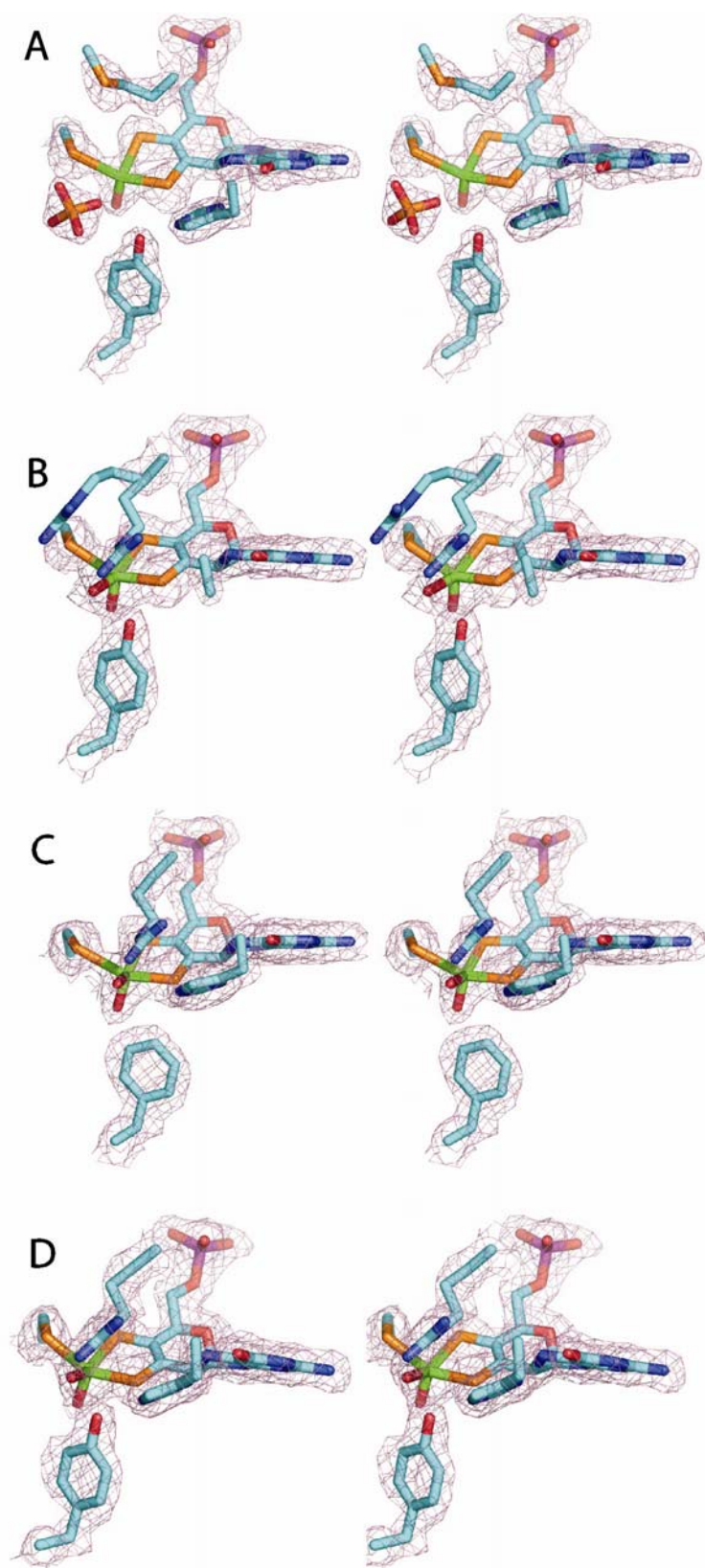


Figure S5